Eastern Anatolian Journal of Science
Volume II, Issue I, 37-48

Present-Day Stress Field in the Bala – Ankara (Turkey) Region from Inversion of Focal Mechanisms

TAHİR SERKAN IRMAK[1,*]
[1]Kocaeli University, Department of Geophysical Engineering,
Seismology Section, 41100, Kocaeli, Turkey

Abstract

The focal mechanisms of the small-moderate earthquakes occurring in the brittle part of the crust are the expression of the present regional stress field and how these stresses act on existing structures in the crust. Especially for the middle and lower crust, for which borehole measurements are not possible, the analysis of focal mechanisms is the only tool for in-situ stress measurements. For this reason, the focal mechanisms of the 2007-2008 earthquakes (23 earthquakes) are obtained from both first motion analysis of vertical P waves (4 earthquakes) and time domain regional body waveforms inversion (19 earthquakes). Using other sources in total 37 earthquake focal mechanisms were obtained to determine active tectonics and the present-day stress field in the Bala-Ankara region. The focal mechanism of the analyzed earthquakes occurred in the Bala-Ankara region obtained both from first motion analysis and time domain moment tensor analysis indicate that the predominant earthquake mechanism is the strike-slip mechanism. All earthquakes occur at shallow depths. Only two events occur at 26 km and 36 km depths. The slip rate is calculated as 0.83 mm/year. The state of recent stress and ongoing deformation in Bala-Ankara region is primarily controlled by the north-northwest drift of the African and Arabian plates respectively. In terms of stress orientations, the Bala-Ankara region is affected by stresses with a general NW-SE orientation of horizontal maximum principal axis (S_{Hmax}N169^{o}E) and NE-SW orientation of minimum principal axis (S_{Hmin}N79^{o}E). However, the extensional features (a few normal faulting focal mechanisms) are observed and these features reflect local stress inhomogeneous compared to the regional stress which is strike-slip.

Keywords: Focal Mechanism, Stress Analysis, Central Anatolia, Bala, Ankara, Turkey.

Accepted Date: 08.04.2016
Corresponding author:
Tahir Serkan Irmak, PhD
Kocaeli University, Department of Geophysical Engineering,
Seismology Section, 41100, Kocaeli, Turkey
E-mail: irmakts@kocaeli.edu.tr

1. Introduction

The tectonic framework of Turkey is dominated by continental collision of the Eurasian and African plates with Eurasia as shown in Figure 1 (MCKENZIE, 1972; JACKSON and MCKENZIE, 1984). The Arabian plate is moving in a north-northwest direction relative to Eurasia at a rate of about 18 mm/yr (MCCLUSKY et al. 2000), averaged over about 3 My based on analysis of global seafloor spreading, fault systems, and earthquake slip vectors. These models also indicate that the African Plate is moving in a northly direction relative to Eurasia at a rate of about 6 mm/yr (MCCLUSKY et al. 2000). Different motions between Africa and Arabia (~ 8-15 mm/yr) are thought to be taken up predominantly by the left-lateral motion along the Dead Sea transform fault. This northward motion results in westward extrusion of the Anatolian Plate (AP). The western part of the AP shows a transition to the Aegean extensional system (AES). The central part of the AP, which the Bala-Ankara region is located there, does not host major faults, and the deformation is seen as internal deformation (ŞENGÖR and YILMAZ, 1981; REILINGER et al. 1997; MCCLUSKY et al. 2000; TAN et al. 2010). Internal deformation includes neotectonic secondary strike-slip faults and extensional basins (BOZKURT, 2001). KOÇYİĞİT and DEVECİ (2008) and KOÇYİĞİT (2009) reported that the direction of compression in the Bala-Ankara region was NW – SE until late Pliocene. The neotectonic regime was initiated controlled by active strike-slip faulting caused by approximately N – S compression. The right and left lateral strike slip faults trend NW – SE and NE – SW, respectively (Fig. 1). The most important structure is the Tuz Gölü Fault Zone (TGFZ) with a mapped length of about 200 km (BEEKMAN, 1966; KOÇYİĞİT and BEYHAN, 1988; ÇEMEN et al, 1999). GÖRÜR et al. (1984) point out that the TGFZ has been active since the Oligocene. There is no reliable historical earthquake information for this area. Also, there is no reliable instrumental period earthquake information until 2005. The 2005 Bala-Ankara earthquake sequence is the first seismic signature well recorded in the instrumental period which is followed by the 2007-2008 earthquake sequence. Both

earthquake sequences are studied by several researchers (ÖZTÜRK and BAYRAK, 2006; KALAFAT et al. 2008; KOÇYİĞİT, 2009; TAN et al. 2010; KORHAN et al. 2011).

Central Anatolia in Turkey is known as a quiet area in terms of seicmicity. The seismicity is characterized by diffused small and moderate earthquakes. Also, numbers of installed stations are less than western part of Turkey resulted less number of recorded earthquakes. Therefore, identification of active fault planes and obtaining detail seismotectonic structures for the area are generally difficult. Such an areas of low-to-moderate seismicity, the small-moderate earthquakes provide the only key to determine fault parameters and small-scale tectonic structure. The focal mechanisms or fault plane solutions of the small-moderate earthquakes occurring in the brittle part of the crust are expression of the present regional stress field and how these stresses act on existing structures in the crust. Thereby, inversions of ensembles of fault plane solutions are useful to constrain the tectonic stress field and allow implications on dynamic processes and on tectonic evolution. Especially for the middle and lower crust, for which borehole measurements are not possible, the analysis of focal mechanisms is only tool for in-situ stress measurements. For this reason, the focal mechanisms of the 2007-2008 earthquakes (23 earthquakes) are obtained from both first motion analysis of vertical P waves (4 earthquakes) and time domain regional body waveforms inversion (19 earthquakes). The focal mechanisms of the 2005 earthquake sequence and data belongs to other instrumental period earthquakes (14 earthquakes) are retrieved from Kalafat et al. (2009) and Tan et al. (2010), respectively. Total 37 earthquake focal mechanisms were obtained to determine active tectonics and the present-day stress field in the Bala-Ankara region. The seismic moments which are obtained from time domain regional waveform analysis are used to determine slip rates for the Bala-Ankara region.

In the simplest approach, *P*, *B* and *T* axes of earthquake focal mechanisms are equated to principal stress axes σ_1, σ_2, and σ_3. In general, if there are pre-existing zones of weakness on which slip occurs, the principal stress axes may not be close to the P, B, and T axes (RALEIGH et al. 1972). MCKENZIE (1969) considered this possibility and showed that the axis of maximum compression may fall anywhere within the dilatational field of the focal mechanism. In such cases, only the direction of resolved shear stress on the fault plane, as indicated by the slip direction, can be used to constrain the stresses. There are many inversion methods in the literature developed to determine the regional stress tensor from an ensemble of earthquake fault plane solutions (e.g. ANGELIER, 1979; ANGELIER et al. 1982; GEPHART and FORSTYH, 1984; MICHAEL, 1984; CAREY-GAILHARDIS and MERCIER, 1987; RECHES, 1987; RIVERA and CISTERNAS, 1990; DELVAUX, 1993; DELVAUX and SPENCER, 2003; IRMAK, 2013; DOĞAN et al., 2016). The inversion method of DELVAUX and SPENCER (2003) was applied to earthquake focal mechanism in this study.

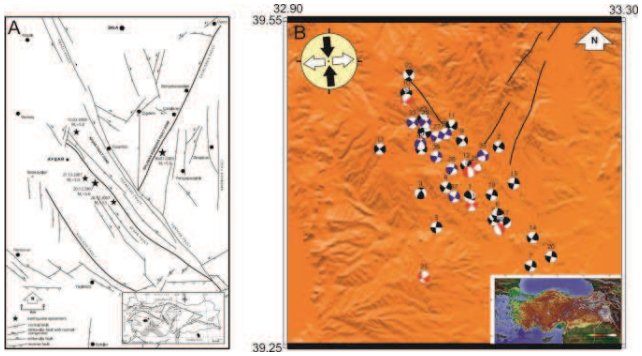

Figure 1A. Inner picture: Simplified map of the tectonics structures in Turkey. The black arrows indicate the motion of the plates. AES: Aegean Extensional System, EAFS: East Anatolian Fault Zone, CAFS– Central Anatolian Fault System, İAESZ– İzmir-Ankara-Erzincan Suture Zone, İEFS– İnonu-Eskişehir Fault System, GV– Galatya volcanics, KOF– Karataş-Osmaniye Fault, NAFS– North Anatolian Fault System, SC– Sakarya Continent, TGFZ– Tuz Golu Fault Zone. Modified from Tan et al. (2010). *Outer picture*: Simplified fault map of the Bala (Ankara) area and its surroundings (modified from Kocyiğit 2009). **B**. Focal mechanisms of studied earthquakes in the Bala-Ankara region. The numbers above the beachballs show event no in Table 1.

2. Data and Methods

Waveform data used in this study were recorded by the Kandilli Observatory and Earthquake Research Institute Seismogical Network. The number of digital broadband stations operated by the National Earthquake Monitoring Center of The Kandilli Observatory and Earthquake Research Institute (NEMC-KOERI) has been increasing since the devastating Kocaeli earthquake of August 17, 1999 in Turkey (IRMAK, 2000). Therefore, nowadays it is possible to obtain reliable fault plane solutions for any area of Turkey using waveform inversion techniques. Digital data sets have been available since 2004 and accessible via the internet provided by the NEMC-KOERI data center.

2.1 First Motion Analysis

The fault plane solutions were calculated by utilizing P-polarities on vertical component seismograms running the *focmec* programs (SNOKE *et al*., 1984) for the analyzed earthquakes. All available polarities from national seismic stations were carefully read. The number of stations with unambiguous first arrival polarities varies from earthquake to earthquake, but events with fewer than 10 clear polarity readings were discarded, as were those with ambiguous polarities. The P-waves were converted to displacement in order to see the P-wave onsets better due to low S/N ratio. Assuming the double-couple model for the seismic point source, P polarities on displacement seismograms were then read. The possible nodal planes which agree with the first motion polarities were searched, running the *focmec* program (SNOKE *et al*., 1984). Polarity errors could be caused by low S/N ratio at stations near nodal planes, so called 'mislocations', or structural heterogeneity, biasing calculation of azimuth and take off angle and aliasing effects (SCHERBAUM, 1994). However, no polarity error was allowed in the solutions. Events with multiple acceptable solutions, indicating different mechanism, or with faulting parameters uncertainties exceeding 20°, were not reported in this study.

2.2. Time Domain Moment Tensor Analysis

Moment tensor analysis theory involves fitting theoretical waveforms with observed broadband waveforms and inverting for the moment tensor elements. A time-domain inverse procedure (e.g., DREGER and ROMANOWICZ, 1994; PASYANOS *et al.,* 1996) was used to estimate the seismic moment tensor of events listed in Table 1. This procedure is designed to obtain reliable solutions using a minimal number of stations. Data from one three-component station would be sufficient, but a few stations with some azimuthal coverage generally give more reliable results. Typically only two or three three-component broadband stations are required to obtain a unique solution (DREGER and HELMBERGER 1993).

In this procedure, the general representation of seismic sources is simplified by considering both a spatial and temporal point-source.

$$U_n(x,t) = M_{ij} \cdot G_{ni,j}(x,z,t) \quad (1)$$

U_n, is the observed n^{th} component of displacement, $G_{ni,j}$ is the n^{th} component Green's function for specific force-couple orientations, and M_{ij} is the scalar seismic moment tensor, which describes the strength of the force-couples. The general force-couples for a deviatoric moment tensor may be represented by three fundamental-faults, namely a vertical strike-slip, a vertical dip-slip, and a 45^0 dip-slip. The indices i and *j* refer to geographical directions. The above equation is solved using linear least squares for a given source depth. In this distribution only the deviatoric seismic moment tensor is solved for, and the inversion yields the M_{ij} which is decomposed into the scalar seismic moment, a double-couple moment tensor and a compensated linear vector dipole moment tensor. The decomposition is represented as percent double-couple (P_{dc}) and percent CLVD (PCLVD). Percent isotropic (PISO) is always zero for this deviatoric application. The double-couple is further represented in terms of the strike, rake and dip of the two nodal planes. The basic methodology and the decomposition of the seismic moment tensor is described in JOST and HERRMANN (1989).

Source depth is found iteratively by finding the solution that yields the largest variance reduction. The results of the moment tensor inversion are generally not very sensitive to location errors. DREGER and HELMBERGER (1993) and also PASYANOS et al. (1996) have shown that errors of up to 15 km in epicenter location are less important at a distance range 50 – 400 km.

It is assumed that the event location is well represented by the high frequency hypocentral location, and a low frequency centroid location is not determined. Second, the simplified representation above assumes that the source time history is synchronous for all of the moment tensor elements and that it may be approximated by a delta function delta since the events used in this study generally have source durations of 2–3 s ($M_L < 5$) (DREGER, 2003).

Preparation of the observed waveforms is a relatively straightforward process involving several steps, which include: 1) removal of the instrument response, 2) rotation of the horizontal components to radial and transverse components, 3) integration to convert to displacement, 4) bandpass filtering: accordingly, $3.5<M_L<4.0$ correspond to the frequency band 0.02-0.1 Hz; $4.0<M_L<5.0$ to 0.02-0.05 Hz; and $M_L>5.0$ 0.01-0.05 Hz, and 5) resampling the data to 2 Hz to match the Green's functions. The Green's functions are also filtered with the same bandpass filter as the observed data.

The quality of the inversion can be controlled by different functions. For instance, a value of 100 of the Variance Reduction means observed and calculated seismograms are identical. Furthermore, the resulting tensor can be decomposed into a double-couple (DC) and a CLVD. The percentage of DC (JOST and HERRMANN, 1989) shows how well the model complies with a double-couple source. However, note that any CLVD contribution is an artifact of the present inversion scheme and indicates influences of structural complexities not considered in the calculation of the Green's functions, source complexities, location errors (depth), etc.

Green's functions were calculated following a modified Haskell algorithm in the frequency–wavenumber domain (SAIKA, 1994). The formulation uses the three basic focal mechanisms (LANGSTON, 1981; HERRMANN and WANG, 1985). Far field and near field terms are both considered by this algorithm. The sampling rate was fixed at 2 Hz. The most important step for the regional moment tensor analysis is developed accurate 1-D velocity model, due to calculate correct Green's functions at regional distances. We used GÜVEN (1999) velocity model as a initial model and a trial and error method that gave the best fit between observed and calculated seismograms was used to adjust final velocity model (Figure 2).

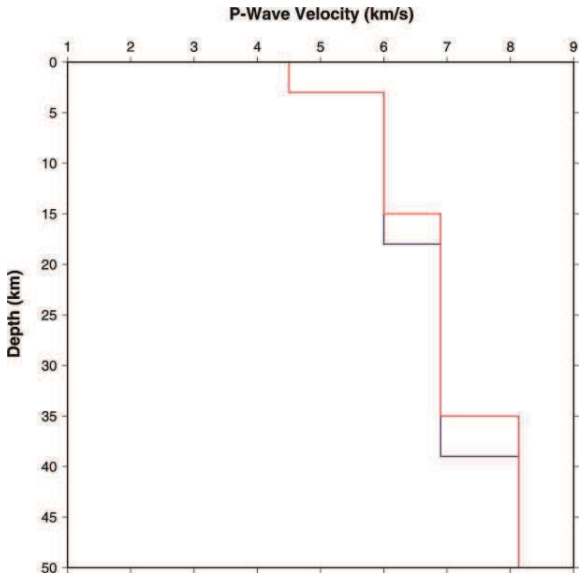

Figure 2. Velocity Model for the Ankara region (modified from Guven, (1999). Blue line shows Guven (1999) model and red is mofified model). Moho depth is 35 km.

2.3. Slip Rate

In this paper, BRUNE (1968) has been followed to calculate the slip rate along the study area. Seismic moments for the earthquakes are calculated from regional waveform inversion. The total average displacement for the whole length of the fault, then, can be calculated from

$$\Sigma \ll u \gg = \frac{1}{\mu A_o} \Sigma M_0 \qquad (2)$$

where u is total average displacement, μ is rigidity, A_0 is fault area and M_0 is seismic moment.

2.4. Stress Inversion

To study the present day stress field for Bala – Ankara region the Win-Tensor program (the new Windows version of the TENSOR program) (DELVAUX and SPENCER, 2003) was performed. The program attempts rely on two major assumptions for the study region: (a) the stress field is uniform and invariant in space and in time, and (b) earthquake slip d occurs in the directions of maximum shear stress τ (Wallace-Bott hypothesis, BOTT, 1959). The angle between the calculated shear stress τ and slip vector d is the fit angle α. Thus, the corresponding misfit function to be minimized for each earthquake i is the misfit angle α:

$$f(i) = \alpha(i) \qquad (3)$$

The orientation of the three orthogonal principal stress axes σ_1, σ_2 and σ_3 (where $\sigma_1 \geq \sigma_2 \geq \sigma_3$) and the stress ratio R:

$$R = \sigma_1 - \sigma_3 / \sigma_1 - \sigma_3 \qquad (4)$$

which expresses the magnitude of σ_2 relative to the magnitude of σ_1 and σ_3.

The data were processed interactively, first using the "Right Dihedron Method", a graphical method for determination of the range of possible orientations σ_1 and σ_3, which is independent from the choice of the nodal planes (ANGELIER and MECHLER, 1977). The initial result is used as a starting point for the iterative grid-search "Rotational Optimization" procedure using the misfit function F5 in the TENSOR program (describes as f3 in DELVAUX and SPENCER, 2003). It minimizes the misfit angle α (Eq.(3)) using the stress tensor that is being tested,

but also favours higher shear stress magnitudes $|\tau(i)|$ and lower normal stress magnitudes $|v(i)|$ on the plane in order to promote slip. It contains three terms and is implemented in a way that it ranges from 0 (optimal misfit) to 360 and is independent from the ratio σ_3/σ_1. The first term that minimizes α is based on the function S4 of ANGELIER (1991):

$$f(i) = sin^2(\alpha(i)/2) \quad (5)$$

and is dominant over the two others (see DELVAUX and SPENCER, 2003 for details).

First we invert both nodal planes for each focal mechanism to a stress tensor. Then the plane that is best explained by the stress tensor is selected from the two nodal planes (smaller value of function F5 in Tensor of f3 in DELVAUX and SPENCER, 2003) and considered as the actual fault (or focal) plane. After this separation, the final inversion then includes only the focal planes that are best fitted by a uniform stress field (GEPHART and FORSYTH, 1984).

In order to express numerically the stress regime, the stress regime index R', based the value of the stress ratio (R, Eq. (4)) and the type of stress regime as described in DELVAUX et al. (1997) and DELVAUX and SPENCER (2003) was used. The tectonic stress regime index R' is defined as:

$R' = R$ for normal faulting regimes (NF)
$R' = (2 - R)$ for strike-slip regimes (SS) and
$R' = (2 + R)$ for thrust faulting regimes (TF)

It forms a continuous scale ranging from 0 to 1 for normal faulting regimes, from 1 to 2 for strike – slip regimes and from 2 to 3 for thrust regimes. The quality evaluation of the results was done using updated quality ranking system of the World Stress Map release 2008 (HEIDBACH et al. 2010). It evaluates the azimuthal accuracy of S_{Hmax} obtained from the formal inversion of N well-constrained single-event focal mechanisms with an average misfit angle α in close geographic proximity (FMF category):

- A – quality (S_{Hmax}/S_{Hmin} within ± 15°): $N \geq 15$ and $\alpha \leq 12^o$
- B – quality (S_{Hmax}/S_{Hmin} within ± 15° – 20°): $8 \leq N \leq 15$ and $\alpha \leq 20^o$ (6)
- C – quality (S_{Hmax}/S_{Hmin} within ± 20° – 25°): not defined for FMF category as individual focal mechanism is assessed to C – quality.

3. Results and Discussions

The focal mechanism of the analyzed earthquakes occurred in the Bala-Ankara region obtained both from first motion analysis and time domain moment tensor analysis indicate that the predominant earthquake mechanism is strike-slip mechanism. All earthquakes occur at shallow depths. Only two events occur at 26 km and 36 km depths.

Figure 3 gives an example of the details of the time domain moment tensor for event no 1 in the Table 1. Data from five of the available stations in the distance range between 250–500 km have been used. Each quadrant has at least one stations means that the azimuthal coverage is good to obtain reliable or stable focal mechanism. Source depth from inversion (12 km) is slightly larger than ISC solution (11 km). Variance reduction is 73% that the correlation of data and synthetics is reasonable. The noise on KDZE station could be reducing the variance reduction value. The double-couple contribution of 78% also indicates a good result. The moment magnitude obtained Mw=4.9 and ISC gives m_b= 5.1. The mechanism indicates strike – slip faulting with *T* axis trending NE – SW and *P* axis NW – SE.

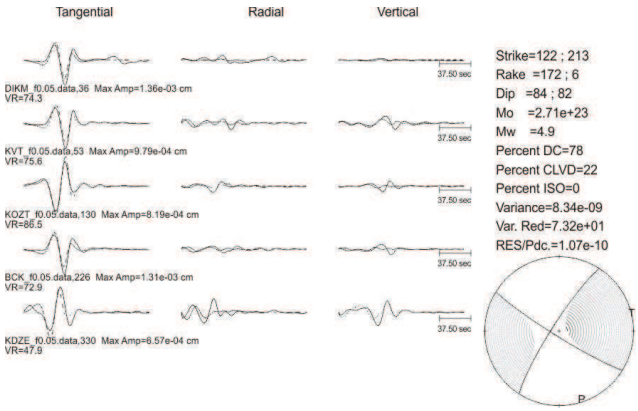

Figure 3. Moment Tensor Inversion results for the event no 1 in Table 1. Dashed: calculated waveforms, solid: observed seismograms; Letters and numbers below seismograms indicate station code, filtered data, azimuth, maximum amplitude and variance reduction value.

Table 1. Source parameters of the analyzed earthquakes.

Event No	Date	Time (UTC)	Lat. (°) (ISC)	Long. (°) (ISC)	Depth (km)	Mw	m_b	Strike1 (^{0})	Dip1 (^{0})	Rake1 (^{0})	Strike2 (^{0})	Dip2 (^{0})	Rake2 (^{0})	P		T		S. Moment (10^{21} dyn.cm)	Comments
														Az	Pl	Az	Pl		
1	20.12.2007	07:36:00	39.3876	33.1182	10	--	3.4^D	100	56	35	349	62	141	46	4	312	47	--	fmp
2	20.12.2007	09:48:27	39.4336	33.1531	11	4.9	5.1	213	82	6	122	84	172	168	1	77	10	271.0	MT
3	20.12.2007	10:16:03	39.3905	33.0596	10	--	3.5^D	224	56	28	218	68	142	274	7	177	42	--	fmp
4	20.12.2007	10:45:52	39.3660	33.1470	5	3.7	3.4^D	212	86	23	120	67	176	344	13	78	18	3.540	MT
5	20.12.2007	10:50:12	39.3587	33.0785	10	3.9	3.6^L	183	83	1	93	89	173	138	4	48	6	8.180	"
6	20.12.2007	11:11:25	39.3712	33.1597	9	--	3.4^D	183	79	27	88	64	168	313	10	48	26	--	fmp
7	20.12.2007	12:34:25	39.3230	33.1912	10	3.6	3.6^D	20	79	-6	111	85	-169	336	11	245	4	3.250	MT
8	20.12.2007	19:18:22	39.3962	33.0898	10	3.7	3.6^D	30	88	-11	120	79	-178	344	9	75	6	4.370	"
9	26.12.2007	23:47:00	39.4392	33.1030	11	4.2	5.1	41	85	19	309	71	175	174	10	266	17	19.70	"
10	27.12.2007	07:47:01	39.4834	33.0423	4	4.1	3.6	237	86	5	147	85	176	12	1	102	6	16.80	"
11	27.12.2007	13:47:58	39.4537	33.0967	13	4.6	4.7	43	77	-27	140	64	-165	359	28	94	8	101.0	"
12	27.12.2007	17:56:12	39.4166	33.1143	10	4.1	4.0^L	27	83	-25	120	65	-172	341	22	76	12	17.10	"
13	28.12.2007	20:57:06	39.4316	33.0108	10	3.7	3.5^L	228	88	3	138	87	178	3	1	94	4	4.330	"
14	29.12.2007	11:54:16	39.3493	33.1937	2	3.5	3.5^D	211	88	23	120	67	178	343	15	78	17	1.940	"
15	04.01.2008	05:03:13	39.3996	33.1711	10	4.2	3.9	9	87	-2	99	88	-177	324	4	234	1	21.00	"
16	07.01.2008	18:26:53	39.4479	33.0633	10	4.0	3.7^L	40	69	-6	132	84	-159	358	19	264	10	10.60	"
17	09.01.2008	09:50:26	39.3630	33.1610	5	--	3.6^D	171	55	33	60	63	140	117	5	22	47	--	fmp
18	11.01.2008	16:07:48	39.4316	33.0604	4	3.9	3.7^D	38	88	-9	128	81	-178	353	8	83	5	8.650	MT
19	14.01.2008	06:57:56	39.3890	33.1448	10	3.8	3.8^L	197	88	2	107	88	178	332	0	62	3	4.980	"
20	20.01.2008	14:45:27	39.3316	33.2157	10	3.5	3.5^D	12	88	1	282	89	178	327	1	237	2	2.160	"
21	26.01.2008	06:57:52	39.4472	33.0653	10	3.7	3.7^D	256	86	9	165	81	176	30	4	121	9	3.720	"
22	01.02.2008	09:11:03	39.4592	33.0625	2	4.1	3.8	50	79	-2	140	88	-169	5	9	274	6	18.30	"
23	15.03.2008	10:15:38	39.5001	33.0455	13	4.9	4.5	142	82	18	50	72	172	275	7	7	18	253.0	"
24	*19.04.1938*	*10:59*	*39.4400*	*33.7900*	*10*	*6.4*	6.8^S	*30*	*60*	*3*	*298*	*87*	*150*	*348*	*18*	*250*	*23*	*49540*	*Kalafat et al (2009)*
25	21.04.1983	16:18	39.3130	33.0636	36	4.8	4.1	64	72	-25	162	66	-160	22	30	114	4	19724	"
26	30.07.2005	21:45	39.4138	33.0970	5	--	5.3^L	24	72	26	285	65	160	153	5	246	31	--	Tan et al 2010
27	31.07.2005	23:41	39.4430	33.0789	5	--	4.8^L	24	80	-5	115	85	-170	340	11	249	4	--	"
28	01.08.2005	00:45	39.4562	33.0651	3	--	4.6^L	42	85	19	310	71	175	174	10	267	17	--	"

D: Duration Magnitude; L: Local magnitude; S: Surface wave magnitude, Italic events did not use in the stress inversion and slip calculation, since they occurred outside of the studied area.

Table 1 (continued)

Event No	Date	Time (UTC)	Lat. (^{o}) (ISC)	Long. (^{o}) (ISC)	Depth (km)	Mw	M_L	Strike1 (^{0})	Dip1 (^{0})	Rake1 (^{0})	Strike2 (^{0})	Dip2 (^{0})	Rake2 (^{0})	P		T		S. Moment (10^{21} dyn.cm)	Comments
														Az	Pl	Az	Pl		
29	06.09.2006	18:47	39.4140	33.1250	10	3.7	3.8	118	65	-20	217	72	-154	79	31	329	4	4.415	Kalafat et al (2009)
30	*21.10.2007*	*21:44*	*39.5570*	*33.1537*	*16*	*4.0*	*3.9*	*335*	*79*	*-89*	*150*	*11*	*-95*	*66*	*34*	*244*	*56*	*10.11*	"
31	23.12.2007	05:02	39.3790	33.1205	26	4.1	3.6^D	221	88	-11	311	79	-178	176	9	267	6	13.85	"
32	19.07.2008	01:27	39.4102	33.1172	4	3.5	3.8^D	176	77	-80	315	17	-130	99	57	258	31	23.22	"
33	23.09.2008	09:09	39.458	33.060	3.2	--	4.7^L	42	80	10	310	80	170	176	1	266	14	--	Tan et al (2010)
34	10.10.2008	06:36	39.4534	33.0432	6	4.2	4.7	49	86	-54	144	37	-173	351	38	108	31	24.31	Kalafat et al (2009
35	31.07.2005	00:45	39.454	33.166	4.2	--	4.2^L	70	90	26	340	64	180	202	18	298	18	--	Tan et al (2010)
36	31.07.2005	15:18	39.436	33.138	3.8	--	4.3^L	17	70	5	285	85	156	333	11	239	17	--	"
37	01.08.2005	02:02	39.400	33.118	3.5	--	4.0^L	28	80	-18	120	80	-170	344	14	74	1	--	"
38	01.08.2005	13:22	39.400	33.133	3.6	--	4.6^L	205	85	10	115	80	175	340	4	71	11	--	"
39	11.09.2008	08:33	39.458	33.060	4.7	--	4.0^L	209	69	-47	320	47	-150	164	48	269	13	--	"

D: Duration Magnitude; L: Local magnitude; S: Surface wave magnitude, Italic events did not use in the stress inversion and slip calculation, since they occurred outside of the studied area.

The results of the stress inversion are shown in Fig. 4. Positions of the principal stress axis are shown in equal-area projections. Since no information about the quality of the fault plane solutions of the earthquakes compiled from different studies, all events from the Bala-Ankara region have been given equal weights in the inversion. The results are represented on map view in function of stress regimes and horizontal stress axes orientation (Fig. 1B).

The inversion results reveal a general trend of NW – SE strike-slip (R'=1.49) movement with a B quality for all over the Bala-Ankara region. The principal stress axes of the best model are oriented close to horizontal (σ_1 (Plunge: 08°/Azimuth: 349°) and σ_3 (Plunge: 00°/Azimuth: 259°)) and vertical (σ_2 (Plunge: 82°/Azimuth: 171°)), also indicating strike-slip regime. The maximum compression axis acts NW – SE direction and the minimum compression axis in a NE – SW direction. The S_{Hmin} orientation is NE – SW almost orthogonal to the Tuz Gölü Fault. These results are agreed with the study of KOÇYİĞİT and DEVECİ (2008) and KOÇYİĞİT (2009).

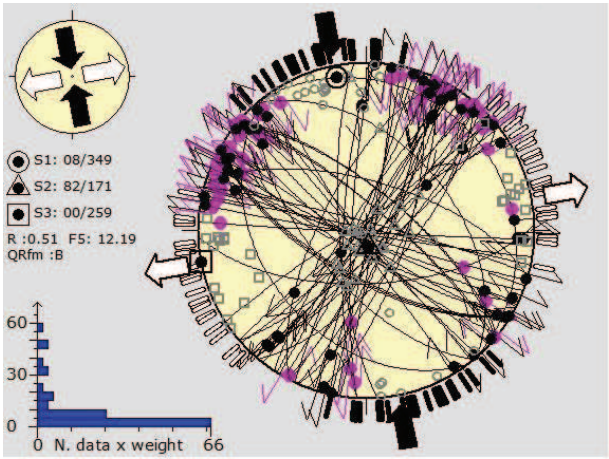

Figure 4. Stress inversion of the focal mechanism data from Table 1. Lower-hemisphere Schmidt stereoplot of the selected focal planes and associated slip lines. Stress inversion results are presented by the orientation of the 3 principal axes (a black dot surrounded by a circle for σ_1, a triangle for σ_2, and a square for σ_3.). The related S_{Hmax} and S_{Hmin} orientations are represented by large arrows outside the stereograms. Their type, length and colour symbolise the horizontal deviatoric stres magnitude relative to the isotropic stress (σ_i) and are in function of the stress regime and the stress ratio $R=\sigma_2-\sigma_3/\sigma_1-\sigma_3$. White arrows and black arrows represents S_{Hmin}, and S_{Hmax}, respectively. The histogram represents the distribution of the misfit function F5, weighthed aritmetically according to the magnitudes.

Although the inversion results indicate that the dominant regime is strike-slip, the 6 focal mechanisms retrieved from Kalafat et al. (2009) are mostly normal faulting (4 events) or strike –slip faulting with normal component (2 events) (Fig. 1B). The focal mechanisms of a few events obtained in this study and retrieved from TAN et al. (2010) have reverse faulting mechanism or strike-slip mechanism with reverse component. Since the occurrence of both normal and reverse faulting is not very likely in a single stress regime, these focal mechanisms suggests that the few normal and reverse events represents local stress inhomogeneous. The large misfit angle, α value indicates the internal heterogeneity (PLENEFISCH and BONJER, 1997). Furthermore, large misfit angles can be caused by badly determined fault mechanisms. PLENEFISCH and BONJER, (1997) used the focal mechanisms to obtain stress field in the Rhine Graben area, and found large misfit angle about 19°-22°. In this study, the misfit angle, α is obtained as 12.19°. For this reason that mentioned above, the focal mechanisms obtained by KALAFAT et al. (2009) were neglected and another inversion with the reduced dataset was done. In comparison to the results of the whole datasets the misfit angle is decreased to 10.56°. For the reduced dataset, the azimuths of the principal stress axes are more or less the same for the whole dataset. The differences between the misfit angles with both data sets are very small and the azimuths of the principal axes are almost same. Therefore, the author suggests that the normal and reverse faulting events represent local stress inhomogeneous. Since all earthquakes occur at shallow depths, change of the stress regime with depth did not investigate. Only two events from 37 events occur at 26 km and 36 km depths. Therefore, the changes in the principal stress axes with depth are not understood.

We took about 30 km to the length of the region and about 10 km to the width of the region using the scale in Figure 1A. Then using calculated seismic moment from Table 1,

$$\Sigma M_0 = 2.0563.10^{17} N.m$$
$$A_0 = 3\ x\ 10^8\ m^2$$
$$\mu = 3.3\ x\ 10^{10}\ Nm^{-2}$$

The total seismic moment is calculated as $\Sigma M_0 = 2.0563 \times 10^{17} N.m$, and the total area is $A_0 = 3.0 \times 10^8\ m^2$, and take the rigidity as $\mu = 3.3\ x\ 10^{10}\ Nm^{-2}$. Then the total slip has been calculated 2.08 cm between the years of 1983-2008. The slip rate for

this period of time is about 0.083 cm/year or 0.83 mm/year using Equation 2.

4. Conclusions

The main objective of this paper is the determination of the present-day stress field in the Bala-Ankara region by the inversion of focal mechanism. Based on reliable 37 fault plane solutions of small-moderate earthquakes obtained from first motion analysis and regional bodywaveform inversion, several inversions runs have been performed using the inversion method of DELVAUX and SPENCER (2003). The predominant earthquake mechanism is strike-slip in the area and all earthquakes occur at shallow depths except two of them located at 26 km and 36 km depths. The slip rate is calculated as 0.83 mm/year. The state of recent stress and ongoing deformation in Bala-Ankara region is primarily controlled by north-northwest drift of the African and Arabian plates respectively. In terms of stress orientations, the Bala-Ankara region is affected by stresses with a general NW-SE orientation of horizontal maximum principal axis (S_{Hmax} N169^{o}E) and NE-SW orientation of minimum principal axis (S_{Hmin} N79^{o}E). However, the extensional features (a few normal faulting focal mechanisms) are observed and these features reflect local stress inhomogeneous compared to the regional stress which are strike-slip. Due to all earthquakes occur at shallow depths, the changes in the principal stress axes with depth are not understood. More data and detailed synthesis may be required for a better understanding of these changing.

REFERENCES

ANGELIER, J. and MECHLER, P., (1977), *Sur une methode graphique de recherche des contraintes principales egalcment utilisable en tectonique et en seismologie: methode des diedres droits.* Bull. Soc. Geol. Fr., 7(19): 1309-1318.

ANGELIER, J., (1979), *Determination of the mean principal direction of stresses for a given fault population,* Tectonophysics 56, T17–T26.

ANGELIER, J., LYBERIS, N., LE PICHON, X., BARRIER, E., and HUCHON, P., (1982), *The tectonic development of the Hellenic arc and the Sea of Crete: A synthesis:* Tectonophysics, v. 86, p. 159–196.

ANGELIER, J., (1991), *Inversion directe et recherche 4-D: comparaison physique et mathernatique de deux methodes de determination des tenseurs des paleocontraintes en tectonique de failles.* C.R. Acad Sci., Paris, 312(11): 1213-1218.

BEEKMAN, P.H. (1966), *Hasan Dağı–Melendiz Dağı bolgesinde Pliosen ve Kuvaterner volkanizma faaliyetleri [Pliocene and Quaternary volcanism in Hasan Dağı-Melendiz Dağı region]*. MTA Bulletin, 66, 88–103 [in Turkish with English abstract].

BOTT, M. H. P., (1959), *The mechanism of oblique-slip faulting*. Geological Magazine, 96, 109-117.

BOZKURT, E. (2001), *Neotectonics of Turkey—A synthesis*, Geodin. Acta, 14, 3–30, doi:10.1016/S0985-3111(01)01066-X.

CAREY-GAILHARDIS, E. and MERCIER, J. L. (1987), *A numerical method for determining the state of stress using focal mechanisms of earthquake populations*. Earth planet. Sci. Lett. 82, 165-179.

ÇEMEN, İ., GONCUOĞLU, M.C. and DIRIK, K. (1999), *Structural evolution of the Tuz Golu basin in Central Anatolia, Turkey*. The Journal of Geology, 107, 693–706.

DELVAUX, D., 1993. *The TENSOR program for reconstruction: examples from the East African and the Baikal rift zones.*Terra Abstracts. Abstract Supplement, 1 to Terra Nova, 5: 216.

DELVAUX D., MOEYS, R., STAPEL, G. et al. (1997), *Paleostress reconstruction and geodynamics of the Baikal region, Central Asia, Part 2, Cenozoic rifting.* Tectonophysics, 282**,** 1-38.

DELVAUX, D. and SPERNER, B. (2003), *Stress tensor inversion from fault kinematic indicators and focal mechanism data: the TENSOR program. In: Nieuwland, D. (Ed.), New Insights into Structural Interpretation and Modelling:* Geol. Soc. Lond. Spec. Publ., vol. 212, pp. 75–100.

DOGAN, B., IRMAK, T.S., KARAKAŞ, A., and KALAFAT, D., (2016), *Seismotectonic content by the source parameters of the June 10, 2012 Ölüdeniz-Fethiye (Dodecanese Islands) Mw6.1 earthquake and afterschocks (southwestern Turkey),* Acta Geod. Geophys., 51, 15-41.

DREGER, D. S., and HELMBERGER, D. V. (1993), *Determination of Source Parameters at Regional Distances with Single Station or Sparse Network Data*, J.Geophys. Res. 98, 8107-8125.

DREGER, D. and ROMANOWICZ, B. (1994), *Source Characteristics of Events in the San Francisco Bay Region,* USGS Open-file report, 94-176, 301-309.

DREGER, D. S., (2003), TDMT_INV: *Time domain seismic moment tensor INVersion*. In International Handbook of Earthquake and Engineering Seismology, ed. W. K. Lee, Boston: Academic Press 81B, 1,627.

GEPHART, J. W. and FORSYTH, D. W. (1984), *An improved method for determining the regional stress tensor using earthquake focal mechanism data: Application to the San Fernando earthquake sequence,* J. Geophys. Res. 89, 9,305-9,320.

GÖRÜR, N., OKAY, F.Y., SEYMEN, İ. and ŞENGÖR, A.M.C. (1984), *Palaeotectonic evolution of the Tuzgolu Basin complex, central Turkey: sedimentary record of a Neo-Tethyan closure*. *In*: Dixon, J.E. and Robertson, A.H.F. (eds), The Geological Evolution of the Eastern Mediterranean. Geological Society of London, Special Publications, 17, 467–482.

GÜVEN, İ. T., (1999), Yapay Sismogram Hesaplama Yöntemi ile Ankara ve Civarının Yerkabuğu Yapısının Modellenmesi, Master Thesis (in Turkish, unpublished).

HEIDBACH, O., TINGAY, M., BARTH, A., REINECKER, J., KURFESS, D., and MILLER, B., (2010), *Global crustal stress pattern based on the World Stress Map database release 2008,* Tectonophysics, 482, 3-15.

HERRMANN, R. B. and WANG, C. Y. (1985), *A comparison of synthetic seismograms*, Bull. Seism. Soc. Am. 75, 41-56.

IRMAK, T.S. (2000). *The source-rupture processes of recent large Turkey earthquakes.* Individual studies by participants to the International Institute of Seismology and Earthquake Engineering, 36, 131-143.

IRMAK, T. S. (2013). *Focal mechanisms of small-moderate earthquakes in Denizli Graben (SW Turkey)*. Earth, Planets and Space, 65(9), 943-955.

JACKSON, J., and MCKENZIE, D. (1984) *Active tectonics of the Alpine-Himalayan belt between Turkey and Pakistan,*Geophys. J. Royal Astronom. Soc. Vol. 77, pp. 185-264.

JOST, M. L., and HERRMANN, R. (1989), *A student's guide to and review of moment tensors,* Seismological Research Letters, 60, 37-57.

KALAFAT, D., KEKOVALI, K., DENIZ, P., GÜNEŞ, Y., PINAR, A., and HORASAN, A., (2008), *31 Temmuz 2005-1 Ağustos 2005 ve 20-27 Aralık 2007 Afşar-Bala (Ankara) Deprem Dizisi (July 31, 2005 - August 1, 2005 and December 20-27, 2007 Afşar-Bala (Ankara) Earthquake Sequence,* İstanbul Yerbilimleri Dergisi, 21(2), 47-60 [in Turkish with English abstract].

KALAFAT, D., KEKOVALI, K., GÜNEŞ, Y., YILMAZER, M., KARA, M., DENİZ, P., and BERBEROĞLU, M. (2009), *Türkiye ve çevresi faylanma-kaynak parametreleri (mt) kataloğu (1938-2008) A Catalogue of Source Parameters of Moderate and Strrong Earthquakes for Turkey and its Surrrounding Area (1938-2008),* Kandilli Observatory and Earthquake Research Institute report.

KOÇYİĞİT, A. and BEYHAN, A. (1998), *A new intracontinental transcurrent structure: the Central Anatolian Fault Zone, Turkey*. Tectonophysics, 284, 317– 336.

KOÇYİĞİT, A. and DEVECİ, Ş. (2008), *Ankara orogenic phase, its age and transition from thrusting-dominated palaeotectonic period to the strike-slip neotectonic period, Ankara (Turkey).* Turkish Journal of Earth Sciences, 17, 433–459.

KOÇYİĞİT, A. (2009), *Ankara'nın depremselliği ve 2005–2007 Afşar (Bala-Ankara) depremlerinin kaynağı [Seismicity of Ankara and source of 2005–2007 Afşar (Bala-Ankara) earthquakes]*. Harita Dergisi, 141, 1–12 [in Turkish with English abstract].

KORHAN, U.S., ÖZEL, N.M., and NECMİOĞLU, Ö., (2011), *Detection and Identification of Low-magnitude Seismic Events near Bala, Central Turkey, Using Array-based Waveform Correlation,* Seism.Res.Lett. 82(1), 97-103.

LANGSTON, C.A., (1981), Source inversion of seismic waveforms: the Koyna, India, earthquakes of September 13, 1967. *Bull. Seis. Soc. Am.*, 71:1-24.

MCCLUSKY, S. et al. (2000), *GPS constraints on plate kinematics and dynamics in the eastern Mediterranean and Caucasus,* J. Geophys. Res., vol. 105, pp. 5695–5719.

MCKENZIE, D. P. (1969), *The relation between fault plane solutions for earthquakes and the directions of the principal stresses,* Bull. Seism. Soc. Am. Vol. 59, no. 2, pp. 591-601.

MCKENZIE, D. P. (1972), *Active tectonics of the Mediterranean Region*, Geophys. J. Royal Astronom. Soc., 30, 109-185.

MICHAEL, A. J. (1984), *Determination of stress from slip data: Faults and folds*, J. Geophys. Res. 89, 11,517-11,526.

ÖZTÜRK, S. and BAYRAK, Y., (2006), *31 Temmuz 2005 Bala (Ankara) depremi, M_D=4.9, artçı şok dizisinin istatistiksel olarak değerlendirilmesi ve artçı şok parametrelerinin bölgesel değişimleri,* Journal of İstanbul Kültür University, 4(2), 145-155. [in Turkish]

PASYANOS, M. E., DREGER, D. S. and ROMANOWICZ, B. (1996), *Towards Real-Time Determination of Regional Moment Tensors,* Bull. Seism. Soc. Am., 86, 1255-1269.

PLENEFISCH, T., and BONJER K. P., (1997), *The stress field in the Rhine Graben area inferred from earthquake focal mechanisms and estimation of frictional parameters.* Tectonophysics, 275, 71-97.

RALEIGH, C. B., HELAY, J. H. and J.D. BREDEHOEFT, (1972), *Faulting and crustal stress at Rangely, Colorado,* in Flow and Fracture of Rocks, Geophys.Monog. Ser., vol. 16, edited by H. C. Heard et al., pp. 275-284, AGU, Washington D. C.

RECHES, Z., (1987), *Mechanical aspects of pull-apart basins and push-up swells with applications to the Dead Sea Transform,* Tectonophysics, 141, 75 – 88.

REILINGER, R.E., MCCLUSKY., S., ORAL, M.B., KING, R.W. and TOKSÖZ, M.N. (1997), *Global Positioning System measurements of present-day crustal movements in the Arabia-Africa-Eurasia plate collision zone.* Journal of Geophysical Research 102 (B5), 9983–9999.

RIVERA, L., and CISTERNAS, A., (1990). *Stress tensor and fault plane solutions for a population of earthquakes.* Bull. Seismol. Soc.Am. 80 (3), 600–614.

SAIKIA, C. K., (1994), *Modified frequency-wavenumber algorithm for regional seismograms using Filon's quadrature; modeling of Lg waves in eastern North America,* Geophysical Journal International, 118, 142-158.

SCHERBAUM, F., (1994), *Basic Concepts in Digital Signal Processing for Seismologists: Springer-Verlag New York, Inc* (Mar 5 1996).

SNOKE, J. A., MUNSEY, J. W. TEAGUE, A. G. and BOLLINGER, G. A. (1984), *A program for focal mechanism determination by combined used of polarity and SV-P amplitude ratio data,* Earthquake Notes 55**,** p. 15.

ŞENGÖR, A.M.C. and YILMAZ, Y. (1981), Tethyan evolution of Turkey: a plate tectonic approach. *Tectonophysics* **75**, 181–241.

TAN, O., et al. (2010), *Bala (Ankara) earthquakes: Implications for shallow crustal deformation in central Anatolian section of the Anatolian platelet (Turkey),* Turk. J. Earth Sci., 19, 449–471, doi:10.3906/yer-0907-1.